A three-degrees-of-freedom motion error measurement system based on interferometry

Qing Yu, Fang Cheng, Hang Su

College of Mechanical Engineering and Automation, Huaqiao University, Xiamen 361021, China

KEYWORDS: Straightness measurement, Phase shift, Mach-Zehnder interferometry, Image processing, Robustness

This paper proposes a three-degree-of-freedom motion error measurement system based on Mach−Zehnder interferometry. The system consisted of an optical flat, beam-splitting prisms, and a reflector. When the stage was moving, the straightness error of the linear guides changed the optical path difference, which in turn caused a phase shift in the interferogram. This phase shift could be calculated by utilizing an image processing algorithm that was also developed during this study. The 3-DOF straightness errors, which included one linear error and two angular errors could be calculated. A commercial laser interferometer and a chromatic confocal sensor were used as reference sensors. The experimental results showed that the linear and angular measurement errors of the system were within ±0.05 μm and ±0.3″, respectively over measurement ranges of 100mm and 60″. The repeatability, which was expressed by the standard deviation, was within 40nm and 0.3″ for the linear and angular measurements, respectively. The proposed Mach-Zehnder interferometer has been successfully applied in a high-accuracy 3D surface topographic measurement system. It was able to effectively compensate the motion error and improve the accuracy for surface profiling..

1. Introduction

When a precision measurement is performed, the linear motion stage, by which the measured sample is carried or driven, provides the basis for linear motion in the ultra-precision measurement system [1, 2]. A straightness error in the motion of this stage is generated by geometric errors produced during component manufacturing and installation. Straightness error measurements are crucial when evaluating the performance of a precision measurement system [3, 4]. Straightness errors can be classified as positioning errors, two different linear errors (unwanted horizontal or vertical motion), or three different three-dimensional angular errors (which include pitch, yaw, and roll angular errors that are measured in arcseconds or microradians) [5, 6]. For surface topography measurement, the most critical motion errors are those that affect the vertical measurement, such as linear error, yaw and roll angular errors.

Currently, straightness error measurement methods can be classified as mechanical measurement methods with mechanical references, optical collimation methods, or laser interferometric methods with lasers as the carriers.

Traditional mechanical measurement methods, such as the leveling method, the wire method, and the micrometer method, are simple and easy to use but are only suitable for low-accuracy applicaitons.

In the optical collimation method, a collimated beam is used as a reference, while quadrant detectors or photodetectors (QDs or QPDs) and position-sensitive detectors (PSDs) are used to capture the motion of light spots induced by the straightness errors. Since PSDs are insensitive to the luminance and shapes of the light spots, self-collimation is suitable for scenarios in which the light intensity varies significantly. However, the measurement accuracy is limited by the detector resolution.

Besides, to measure straightness errors with more than one DoFs, multiple sensing units were needed. In some cases, even multiple sensing techniques were involved. During this study, an improved measurement system, which was based on Mach-Zehnder interferometry and could simultaneously measure 3-DOF motion errors of the linear guide, was developed. The motivation of this study was to provide a compact straightness measurement system, which can be integrated easily into a precision measurement system. With this system, the interferometer could be installed such that there was a significant standoff with respect to the moving stage. The developed system can effectively compensate for motion errors in the z-direction, which is the most important factor in surface topography measurements.

2. Measurement Principle

Fig. 1(a) shows the principle of Mach-Zehnder interferometry. It was firstly proposed in 1891 and now is widely used in quantum physics study, temperature sensing, refraction measurement, etc. Fig. 1(b) presents a schematic of drawing of the motion error measurement system proposed by the authors' team. The measurement system primarily consisted of a linear stage, an optical flat, two beam splitting prisms, a reflector, a semiconductor laser, and an image acquisition module. In this system, the optical flat and the reflector were not perfectly parallel. A small angle was set between them to generate an initial interferogram. With an appropriate incidence direction, the light emitted from the light source was split into two beams by one of the beam-splitting prisms. One beam was directed toward the optical flat, while the other beam was directed toward the reflector. After being reflected by the optical flat and the reflector, the two beams met at the second beam-splitting prism and generated an interferogram on the screen. During the motion, the interferogram would show that a phase shift was associated with the straightness error of the linear stage. An image processing algorithm, which was developed by the authors, was then used to calculate the 3-DOF straightness error, the standoff variation, the roll error and the yaw error.

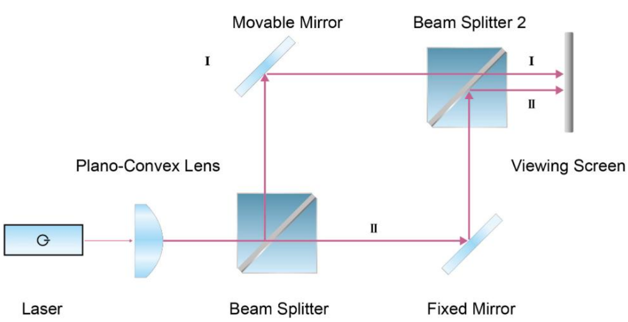

(a) The principle of Mach-Zehnder interferometry

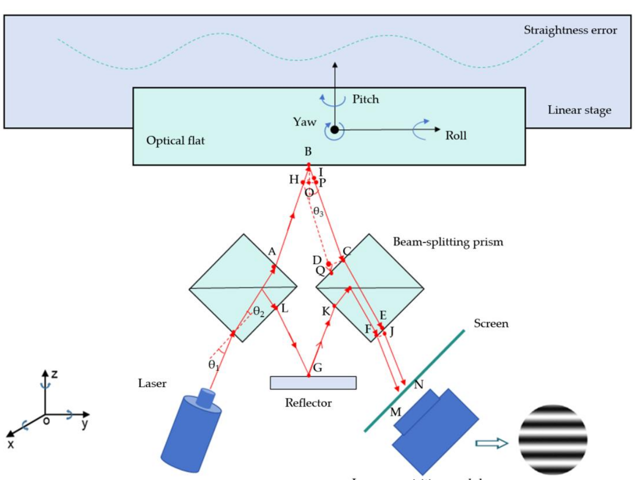

(b) Schematic diagram of the intereference module

Fig. 1 Schematic diagram of the interference module

The straightness error generated during the motion of the stage can be divided into linear errors and angular errors. According to the conclusion presented above, k is not affected by the angular errors. To verify this conclusion, a simulation was conducted using the Zemax software. Various angles were utilized during the simulation process, and the linearity coefficient was calculated with an algorithm that was developed based on connected domain extraction. The simulation results presented in Table 1 show that the angular motion error changed the spacing and orientation of the interference stripes. Figure 2 indicates that the linearity coefficient between the distance variation and the phase shift of the interferogram remained unchanged under the effects of different angular errors. Additionally, the figure demonstrates that the angular errors did not affect the linear error measurement method.

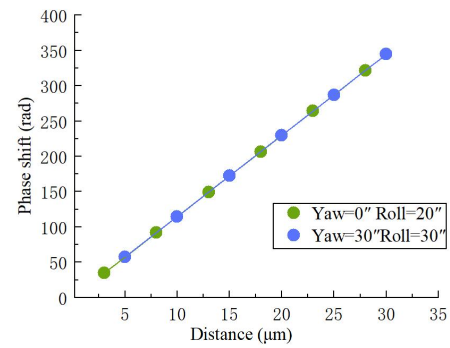

Fig. 2 Relationship between the phase shift and the distance at different angles.

Table 1 Angle variations and interferograms

Roll \ Yaw	0″	10″	20″	30″
0″				
10″				
20″				
30″				

.

3. System Development

To verify the performance of the linear straightness error measurement method proposed, a linear motion error measurement platform was assembled, as shown in Figure 3. The primary specifications of the main components are listed in Table 2.

Table 2. Primary specifications of the main measurement platform components.

Component	Type	Specifications
Light source	RiCheng Technology RP635-50G11	Power: 50 mW Wavelength: 650 nm Spot diameter: 10 mm
Beam-splitting prism	HengYang Optics	Material: K9 glass Flatness: ≤0.06 μm Dimensions (mm): 12.5 × 12.5 × 12.5

Optical flat	Sanfeng Standard Measuring Implements	Material: K9 glass Flatness: ≤0.05 μm Dimensions (mm): 120×30×25
Linear stage	Zolix CXPF100-80175	Travel range: 100 mm Positioning accuracy: ≤ ±2 μm Straightness: ≤ 10 μm
Chromatic confocal sensor	Precitec CHRocodile SE	Measurement range: 600 μm Linearity error: < 0.2 μm Resolution: 3 nm
Lens	MORITEX ML-MC50HR	Magnification: 0.5~0.8 Focal distance: 50 mm Working distance (mm): 149–111
Camera	Basler a2A4200-12gm	Sensor format: 2/3" Frame rate: 12 fps Resolution: 4200 × 2610

As shown in Figure 3, the optical flat was mounted as a geometric reference on the linear stage to be measured. The optical flat was angled with respect to the reflector such that the beam created interferograms at the screen. The linear stage was driven by an MC600 controller. CHRocodile SE color confocal sensor from Precitec was used as a reference sensor for linear motion error measurements. The sensor has a working distance of 6.5 mm, and the nonlinear error can be controlled below 0.2 μm in the 600 μm measuring range. Since up to 5% of the measuring range (30 μm) is used in the experiments, the nonlinear error within 30 μm should be much less than 0.2 μm. With submicron accuracy, the CHRocodile SE was used as a reference sensor for the linear motion error for comparison study in this project.

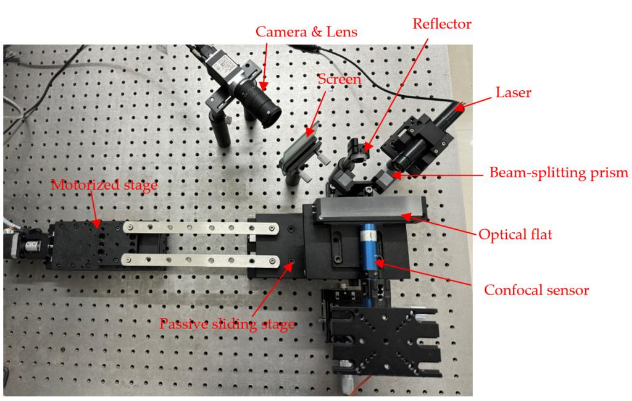

Fig. 3 Linear straightness error measurement platform

As shown in Figure 4, two experimental platforms were assembled to measure the angular motion error. The Keysight 5530 laser interferometer produced by Agilent was used as a reference sensor to record the angular variations. Its angular measurement accuracy for the display value of ±0.2%, resolution up to 0.05″. Notably, the Keysight 5530 is capable of measuring angular motion errors from 2 DoFs while the stage is in motion. There are 3 laser beams from the interferometer, measuring the linear displacements along 3 parallel lines. The differences among these 3 linear displacements will be used to calculate the angular motion errors.

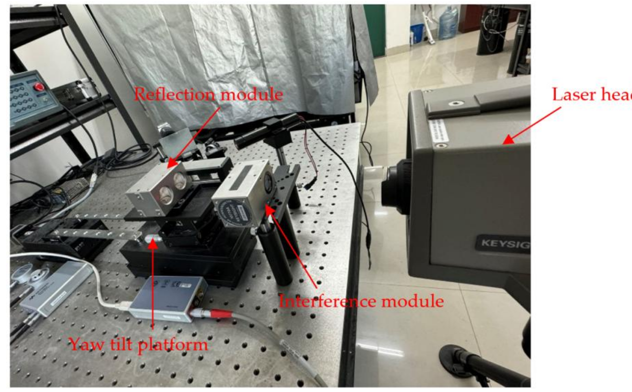

(a) Yaw angle motion error measurement platform

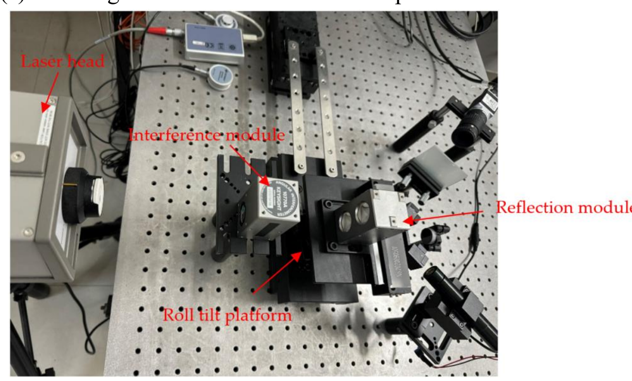

(b) Roll angle motion error measurement platform

Fig. 4 Angular motion error measurement platform

4. Experimental Results

For the linear straightness error measurement experiment, the measurement range was set to 100 mm with a sampling increment of 1 mm. A chromatic confocal sensor was used to record the distance variation. Due to installation deviations, the motion paths of the optical flat and the displacement stage were not completely parallel. Thus, the distance variation was caused by the superposition of the coaxiality and straightness errors, as shown in Figure 5(a). The straightness error was obtained by subtracting the coaxiality error from the distance variation. As shown in Figure 5(b), the linear straightness error was 12 μm. Moreover, Figure 5(c) shows that the measurement deviation between the measurement system developed during this study and the chromatic confocal sensor was within ±0.05 μm, while the standard deviation was within 40 nm.

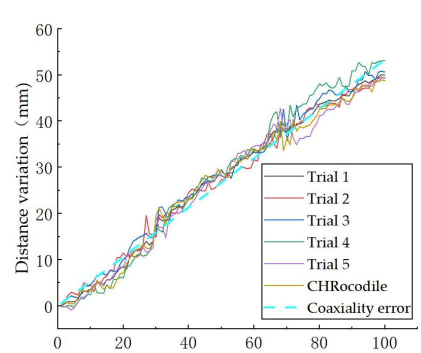

(a) Distance variation

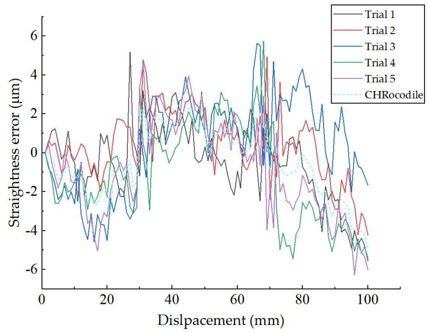

(b) Straightness error

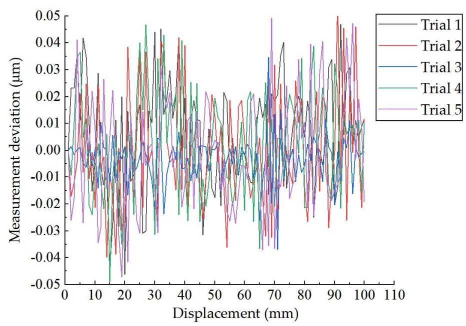

(c) Measurement deviation

Fig. 5 Results of the linear motion error measurement experiments

The experiment was repeated five times each for the yaw and roll angles. The travel range was 60’’ and an increment of 10’’ was achieved by a precision goniometer. In Figure 6, the blue dots represent the arithmetic mean of the measurement deviation at each sampling point, and the error bars represent the standard deviation. The results show that the maximum measurement deviation between the laser interferometer and the proposed system was within ±0.3’’, while the standard deviation was within 0.3’’. This measurement deviation includes the measurement uncertainty of the laser interferometer. Therefore, the two metrics discussed above represent a conservative performance evaluation of the proposed system.

The experiment was repeated five times each for the yaw and roll angles. The travel range was 60’’ and an increment of 10’’ was achieved by a precision goniometer. In Figure 6, the blue dots represent the arithmetic mean of the measurement deviation at each sampling point, and the error bars represent the standard deviation. The results show that the maximum measurement deviation between the laser interferometer and the proposed system was within ±0.3’’, while the standard deviation was within 0.3’’. This measurement deviation includes the measurement uncertainty of the laser interferometer. Therefore, the two metrics discussed above represent a conservative performance evaluation of the proposed system.

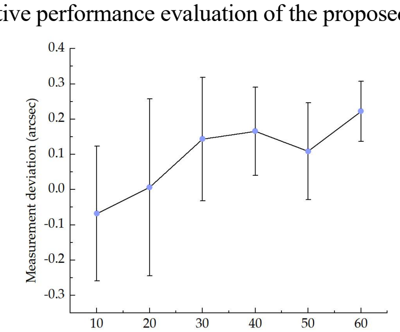

(a) Measurement deviation for yaw angle motion errors

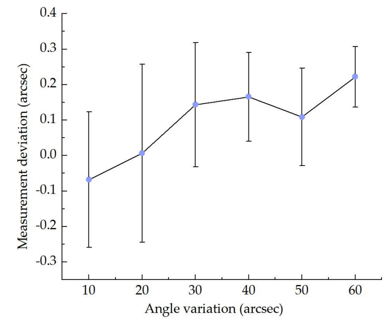

(b) Measurement deviation for roll angle motion errors

Fig. 6 Angular motion error measurement results

5. Conclusion

In this study, a 3-DOF motion error measurement system based on Mach–Zehnder interferometry was developed to measure the straightness error of a precision linear motion stage.

In this system, the beam was split by a beam-splitting prism, after which it was reflected by an optical flat and reflector to produce an interferogram. After the relation-ship between the phase shift and the standoff variation was derived, a phase shift algorithm, which was developed based on connected domain extraction, was used to calculate the phase shift of the interference stripes. Then, the linear straightness error and the angular straightness errors (which included yaw and roll errors) could be obtained.

ACKNOWLEDGEMENT

This study was supported by the National Natural Science Foundation of China (No. 52075190 and No. 52211530491); the Science and Technology Projects of Fujian province, China (No. 2023I0017).

REFERENCES

1. He Y X, Lin R W, Li R J, et al. “Nanopositioning X–Y stage with an embedded Six-DOF error compensation system based on Abbe and Bryan principles,” *Measurement*, Vol. 227, pp. 114218, 2024.
2. Wang J, Zhao W, Leach R, et al. “Positioning error calibration for two-dimensional precision stages via globally optimized image registration,” *Measurement*, Vol. 186, pp. 110222, 2021.
3. Xu X, Tan Y D, Mu H L, et al. “Laser Interferometric Multi-Degree-of-Freedom Measurement Technology in Space Gravitational-Wave Detection,” *Laser & Optoelectronics Progress*, Vol. 60, No. 3, pp. 0312006, 2023.
4. Wu Z J, Zhang Q C. “High-Speed 3D Topography Measurement Based on Fringe Projection: A Review,” *Laser & Optoelectronics Progress*, Vol. 60, No. 8, pp. 0811001, 2023.
5. Tan Y D, Xu X, Zhang S L. “Precision measurement and application of laser interference,” *Chinese Journal of Lasers*, Vol. 48, No. 15, pp. 1504001, 2021.
6. Elmelegy A, Zahwi S. “Comparative study of error determination of machine tools,” *The International Journal of Advanced Manufacturing Technology*, Vol. 124, No. 11, pp. 4575-4602, 2023.